# Time Series Analysis of the Digital Elevation Model of Kuwait Derived from Synthetic Aperture Radar Interferometry

K.S. Rao and Hala K. Al Jassar

Physics Department, Kuwait University, P.O. Box 5969, Safat 13060, Kuwait
{ksrao,hala}@kuc01.kuniv.edu.kw

**Abstract.** The digital elevation model derived from SAR Interferometry is prone to atmospheric, penetration into soil medium, system noise and decorrelation errors. Eight ASAR images are selected for this study which have unique data set forming 7 InSAR pairs with single master image. It is expected that all the DEMs should have the same elevation values spatially with in the noise limits. However, they differ very much with one another beyond the noise levels indicating the effects of atmosphere and other disturbances. The 7 DEMs are compared with the DEM of SRTM for the estimation of errors. The spatial and temporal distribution of errors in DEM are analyzed by considering several case studies.

**Keywords:** Digital Elevation Model, SAR Interferometry, phases, penetration depth.

## 1 Introduction

Synthetic Aperture Radar Interferometry (InSAR) is a powerful technique for deriving Digital Elevation Models (DEMs) with high spatial (a few tens of meters) and vertical (a few meters) resolutions [1,2] . The operational satellite systems such as Environmental satellite (ENVISAT), European Remote Sensing Satellite (ERS), Radar Satellite (RADARSAT), Japanese Earth Resources Satellite (JERS) etc., provide SAR data suitable for repeat pass InSAR. The repeat pass InSAR has limitations in deriving accurate DEM due to tropospheric phase delay as has been reported by several authors in the past [3, 4]. In view of several applications of DEM, both civilian and defense, there is an interest to develop models to minimize the tropospheric errors in repeat pass InSAR.

Kuwait, being a desert, has additional problems. The desert sand, being completely dry, allows microwaves to penetrate into the soil medium. The penetration depth depends on soil moisture. The annual variation of soil moisture over Kuwait desert will be from 3% to 10% by volume. Therefore, the measured phases in different SAR scenes used in repeat pass InSAR will be diffused leading to more errors in the derived DEM. Kuwait desert has some specific features such as scattered settlements, grazing of sheep, wind blow. These features will disturb the top soil layers leading the decorrelation of phases of the two SAR images used in repeat pass InSAR.

K. Sithamparanathan et al. (Eds.): PSATS 2010, LNICST 43, pp. 396–406, 2010.

The climate of Kuwait desert is arid with very hot dry summers and mild rainy winters [5]. There are generally four seasons in Kuwait: winter, spring, summer and autumn, within are several seasons. Sub-seasons are periods of distinct weather, such as frequent dust storms. Winter is the wettest and coldest season and begins in December and ends in mid-February. Spring begins in by mid-February and generally last through May. The temperatures vary between – 4.0° C to +50° C. The mean annual rainfall is 115 mm with variability from year to year (28-260 mm) and from place to place. There are no rains during the period May – October.

## 2 ASAR Data and DEM of SRTM

On March 1, 2002 ENVISAT satellite was launched by an Ariane 5 launcher. Among several payloads, ASAR is one of the main instruments on board ENVISAT satellite. ASAR images the land at C-band (5.3 GHz or 5.63cm) with choice of 5 polarizations and 3 modes (http://envisat.esa.int /instruments/asar/). Through a project (C1F-3807) sponsored by European Space Agency (ESA), we have been receiving ASAR data in Single Look Complex (SLC). We started receiving the data since the year 2005 and by now we have 29 scenes. The data is acquired in the descending mode for the track /swath no (464/I1) at VV polarization.

The basis for selecting ASAR data for generating DEM is the $B_\perp$. The relation between $B_\perp$ and its sensitivity to topography is given in [6] and the simplified form is as follows:

$$h = \frac{\lambda r \sin\theta}{4\pi B_\perp}\varphi$$

where h is the topographic elevation, λ is the wavelength, r is the range from satellite to the ground pixel, θ is incident angle, and $\varphi$ is the interferometric phase. The height per fringe ($h_a$) is given by

$$h_a = \frac{\lambda r \sin\theta}{2B_\perp}$$

Therefore, higher $B_\perp$ means more sensitive to elevation. At the same time, very large $B_\perp$ leads to de-correlation of interferometric phases. Therefore, $B_\perp$ in the range 200 m – 400 m is selected for this study. Following the above condition, 7 pairs are possible with one master image of December 2007. Though we generated all the DEMs, in this study we are discussing only these 7 DEMs. Since the master image is common for all these DEMs, they are automatically registered and so direct comparison is possible without separately registering them with one another.

### 2.1 DEM of SRTM with 90 m Spatial Resolution

Ninety meter spatial resolution DEM generated from SRTM is freely available in the internet. DEM of 90 m spatial resolution is downloaded from the site http://srtm.sci.cgiar.org/ and used in this study as a reference. DEM of SRTM will be registered and re-sampled to ASAR resolution so that it can serve as a standard reference for error analysis of DEM of repeat pass InSAR. Though the topography of

Kuwait desert is flat and gently sloping down towards west, Burgan oil field has a ridge of 120 m height extending North – South direction.

The DEM of SRTM is one of the best data sets available freely to the scientific community. This has been extensively validated and used for many scientific publications [7]. To assess the elevation accuracy of DEM of SRTM over Kuwait Desert terrain, it is compared with spot values (benchmarks) given in topographic map of Kuwait. RMSE for DEM of 90 m is 3.3 m and RMSE for DEM of 50 m is 1.7 m. Since there is a large gap in time between SRTM and survey of Kuwait topographic map, it is quiet possible that some locations might have been disturbed.

## 3 Generating DEM Using Repeat Pass InSAR Technique

The flowchart for generating DEM is shown in Figure 1. GAMMA interferometric modules are used for generating DEM of Kuwait. A brief description of various steps shown in flowchart are explained here. A rough estimate of offset between the two ASAR images (master and slave images) is done at Multi Look Intensity (MLI) image by averaging 2 range x 10 azimuth pixels and it is fine tuned at Single Look Complex (SLC) using intensity cross-correlation approach with search window 64 x 128 pixels. The slave (second) image is registered (by identifying 48 x 48 registration locations equally distributed through out the image) with master (first) image.

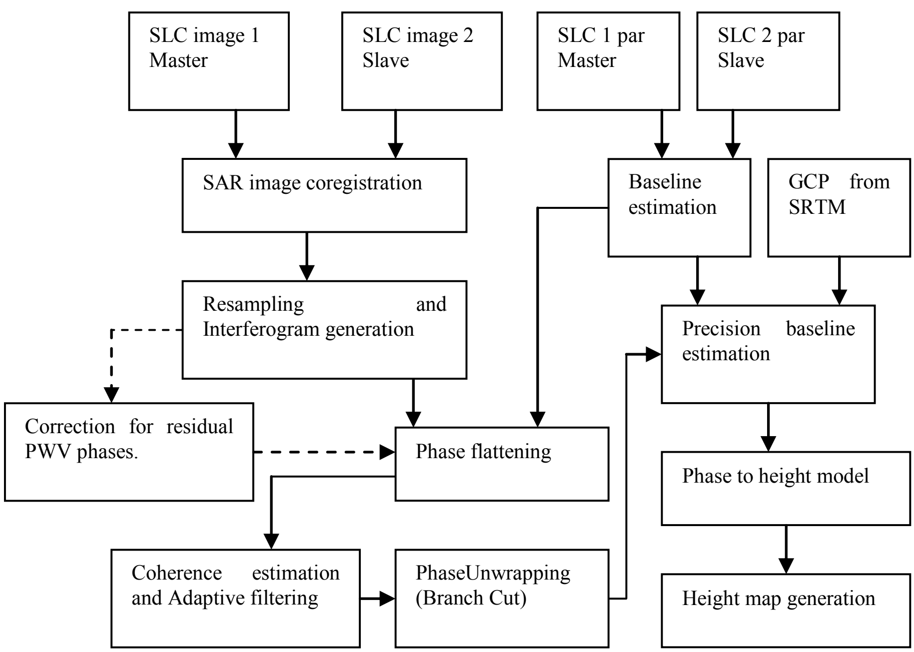


**Fig. 1.** Flow chart for generating DEM through InSAR including PWV corrections

Initial baseline is estimated using state vectors and then refined using 99 Ground Control Points (GCPs) obtained from DEM of SRTM. The spatial distributions of GCPs are shown in Figure 10. It can be seen from Figure 10 that the GCPs form two groups; one corresponding to Burgan oil field and another Manaqish (Umm Qudayr) oil fields. Though the study area is only Burgan, the GCPs are selected over other oil fields for better accuracy. Outside the oil fields (in the open areas), the interferometry was not possible due to decorrelation of the phases.

Phase unwrapping is performed after removing the flat terrain fringes (estimated based on $B\perp$), applying adaptive filtering and estimating coherence. Branch Cut (BC) approach followed by bridges is used for phase unwrapping. Finally the interferometric phases are converted into elevations using phase – height model. The baseline components and their variation with azimuth are estimated using least square approach.

## 4 Results and Discussions

There are several reasons for the errors in repeat pass InSAR such as (1) different models used in processing ASAR data, (2) instrument noise, (3) error in baseline estimation, (4) atmospheric water vapor and clouds, (5) desert dry soil penetration of the microwaves, etc.

### 4.1 Temporal and Spatial Comparison of Errors in Different DEMs of Burgan Oil Filed

While processing the data sets, several problems were encountered. Since Kuwait is a desert area, the sand moves frequently destroying the phase coherence even with the day difference of 35 days. From the phase coherence point of view, Kuwait can be classified as three main classes namely built-up city areas, open areas and protected areas. All the installations and Oil fields are protected with a metallic wire fence. The open areas are the places where scattered settlements are seen and grazing takes place. City areas having buildings show high phase coherence; fenced areas with least disturbance have good phase coherence where as open areas have low phase coherence. Figure 2 shows the visible image of Kuwait and the protected areas.

Therefore, interference fringes are formed only on the protected areas such as oil fields and built-up city areas. Several processing parameters in GAMMA modules are adjusted to get the best results. Also the threshold limit for signal to noise is adjusted for best registration of the two images selected to eliminate weak registration points where the signal strength is very low. 99 GCSs are selected covering uniformly both the main oil fields of Kuwait to help in precession estimation of baseline components and their variation with azimuth. The elevations of these GCPs are extracted from the 90 m spatial resolution DEM of SRTM after resampling and registering with ASAR image.

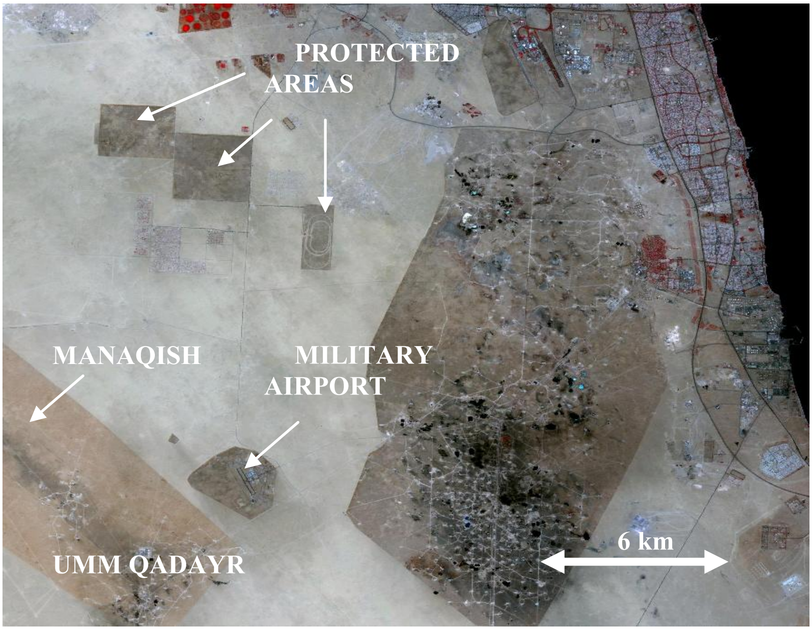


**Fig. 2.** TM Landsat-7 image of Kuwait oil fields. Band 2 (R), Band 3 (G), Band 4 (B)

To highlight the errors in the DEM generated through repeat pass InSAR, 90 m DEM of SRTM is transformed into ASAR geometry and registered with InSAR DEM and then subtracted. Since DEM of SRTM is free from atmospheric and other (penetration of waves into desert sand etc.,) errors as both the images are acquired simultaneously, it is taken as a reference in this study. Figures 3a-g show errors (subtraction of DEM of repeat pass InSAR from DEM of SRTM) in seven DEMs of Burgan. Table 1 gives RMS and STD errors considering the entire oil field and at two distinct locations indicated in Figure 3a. It can be seen from Table 1 that STD and RMS values are more or less same. This is because the mean error is close to zero. The STD is to know the variance in the errors where as RMS is a measure of the deviation of InSAR DEM from the DEM of SRTM. The mean error is close to zero indicates that there is no bias between DEMs of SRTM and InSAR. The STD values vary from 2.2 to 9.4 m. The spatial and temporal distributions of errors are evident from Figures 3a-g. They are arranged in the increasing order of day-diff. The colour coading is done in the interval of 3 m as shown in Figure 3. The gray colour all around Burgan oil field in Figure 3 refers to low phase coherence and so they are made as Zeros just to exclude for the analysis.

- Figure 3a shows the spatial distribution of errors for the interferogram of 35 day difference having a phase coherence of 0.93. It can be seen from Figure 3a that errors over Burgan oil field are mostly within ±3 m. However, on the southern side, it shows a high gradient with an error poorer than -10 m. Similarly, on the left – middle portion, brown colour indicates the range of 3 to 6 m. The average error is only -0.38 with STD of 3.8 m.

**Table 1.** Errors in elevation values (in m) for two locations P1 and P2. Also for the entire study area Burqan. The common master image is of Dec. 2007. The RMS and STD are same (upto one digit after the decimal point) for most of the cases where the mean error is close to zero.

| DEM pair | Day-diff | P-1 | P-2 | RMS |
|---|---|---|---|---|
| October 07 | 35 | -1.32 | 0.28 | 3.8 |
| August 07 | 105 | 0.17 | -0.01 | 2.5 |
| July 07 | 140 | -0.09 | -0.43 | 2.2 |
| June 07 | 175 | -2.16 | 3.14 | 3.8 |
| January 07 | 315 | -3.56 | 0.57 | 5.3 |
| September 06 | 455 | -0.08 | -3.48 | 5.4 |
| June 06 | 525 | 5.63 | -6.45 | 9.8 |

- There is a good consistency in the values of Figures 3b and 3c where the RMS error is only 2.5 m and 2.2 m respectively. Also the errors are in the range of ±3 m (blue and green colours and a few locations brown colour. 105 and 140 days are the day-diff in these two cases. The coherence (0.9 and 0.89) is also very high.
- Figure 3d corresponding to 175 day difference shows values in the range -3 m to 10 m at some locations, though the overall range is ±3 m. There is no definite trend in the results. The average value is 0.36 m with RMS of 3.8m
- Figure 3e corresponds to 315 day difference shows values varying in the range ±10 m. The trend resembles to some extent with Figure 3a in the southern portion of Burgan. Though the average error is only 0.31m, the STD is 5.33 m. The average coherence in this case is 0.72.
- Figure 3f refers to day-diff of 455 days which has least errors in the middle portion of oil field. On the southern side, the values are positive and turned to negative around Northern side. In this case, the average coherence is 0.75. The mean value is 2.16 m with STD of 4.9 m.
- Figure 3g corresponds to 525 day difference is the worst of all the others. Though the average error is 2.55m, the STD is as high as 9.4 m with a coherence of 0.69.

In general, there is no either spatial or temporal consistency in the errors (Figure 3). However, the errors within ± 3 m should not be taken into account as the reference DEM of SRTM itself has an error of this order. In this respect, the central portion of Burgan oil field has errors within the limits in most of the cases.

Figures 3b and 3c are very good. Figures 3a, 3e and 3g show vertical fringe like patterns with large errors on the Southern portion of the oil fields. To some extent, the range of errors increases with day-diff after a particular period which in turn has effect on coherence, there is no consistency in the spatial distribution. Since water vapour and soil moisture patterns are very dynamic in spatial variations, the observed trends can be understood in these terms. The RMS error does not seem to be a good indicator of overall errors. Even though the spatial distribution of errors in some pockets of the study area are as high as 10m, the RMS value is still very low as the percentage of these pixels does not influence the RMS considerably.

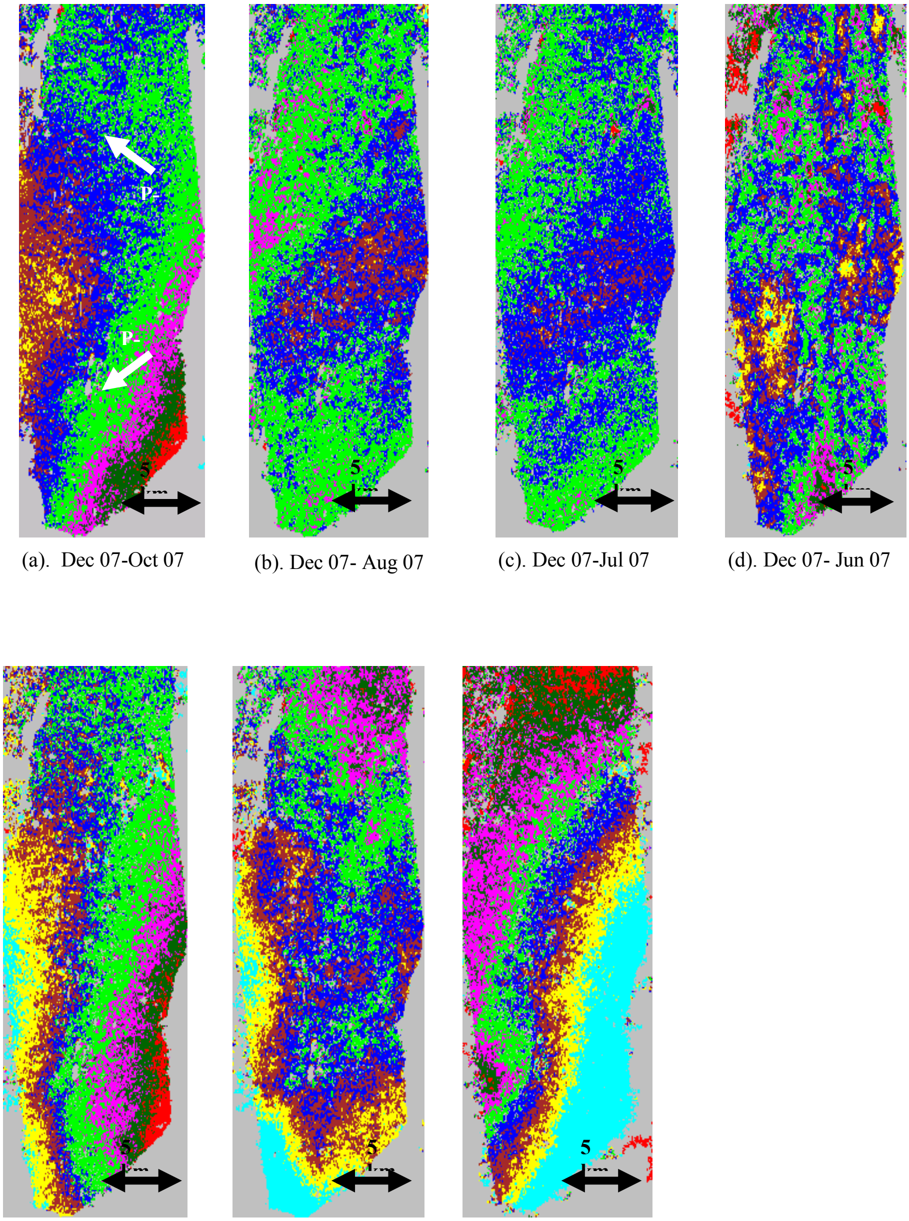

(a). Dec 07-Oct 07 (b). Dec 07- Aug 07 (c). Dec 07-Jul 07 (d). Dec 07- Jun 07

(e). Dec 07- Jan 07 (f). Dec 07- Sep 06 (g) Dec 07- Jun 06

**Fig. 3.** Errors in the DEM of Burqan (SRTM- InSAR)

### 4.2 Study on the Quantitative Consistency of the Elevations

Since the errors in the derived DEMs are varying spatially and temporarily, it is worthwhile to go for a quantitative analysis of these errors. Therefore, two specific locations are selected as shown in Figure 3a : One location P1 at the southern portion of the oil field and the other P2 at the Northern portion of the study area. Figure 4 shows the errors as a function of day difference for points P1 and P2. It can be seen from Figure 4 that there is not much consistency in the results as a function of time. The errors are in the range ±6 m.

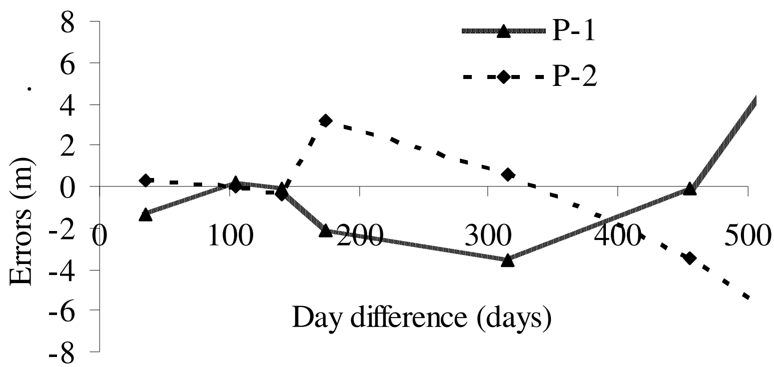


**Fig. 4.** Elevation as a function of Day-diff for two selected points in Burqan oil field

### 4.3 Relation between Day-Diff, Coherence and RMS Errors

To investigate into the other possible reasons of the errors in the DEMs, average coherence is plotted as a function of day-diff as shown in Figure 5a. The coherence steadily decreases with increase in day-diff. Second degree polynomial shows better fitting with the data. The equation of fitting is given in the figure itself. Since the study area is protected, desert and no human activities, the coherence is not supposed to decrease with day-diff. The observed decrease can be due to the change in vegetation cover which is protected from the cattle grazing. As the day-diff increases, some changes are natural to take place on the ground in terms of vegetation cover.

Figure 5b shows the RMS error as a function of day-diff. Except a few cases, the RMS error steadily increases with day-diff. Since coherence has an effect on the reliability of the phases, the decrease of coherence leads to increase in RMS error. The observed linear relation may not hold for higher day-diff. Similarly Figure 5c shows the relation between RMS error and the average coherence which is self explanatory.

### 4.4 Effect of Variation of Soil Moisture on the Accuracy of DEM

The presence of precipitable water vapour in the atmosphere delays the microwave signals. The differential delays causes errors in the elevation data. Atmospheric corrections are implemented for the DEMs using the models reported by [4]. MERIS PWV is used for the corrections. It has been noticed that the corrections did not improve the results as the variation of PWV over desert is seen to be not significant.

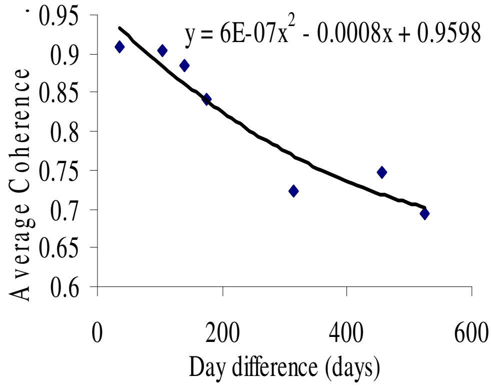


**Fig. 5a.** Relation between Day difference and Coherence

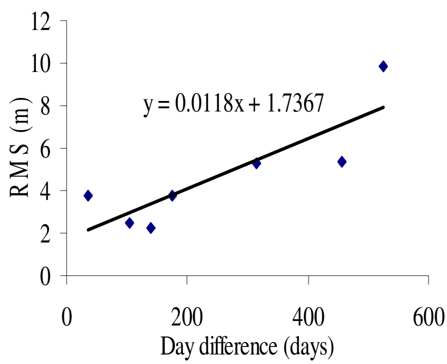


**Fig. 5b.** RMS error as a function of Day difference

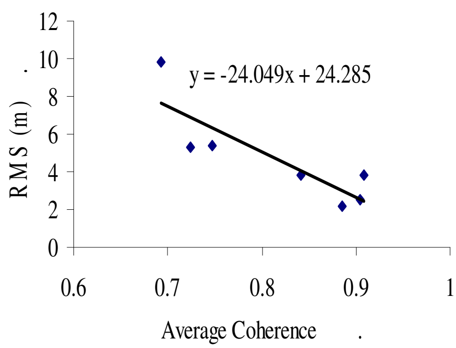


**Fig. 5c.** Relation between RMS error and Coherence

The processing steps are checked again and again to make sure that there are no errors in generating repeat pass DEM. The speckle and instrument noises are minimized by averaging the pixles to a resolution of 60 x 60 m and by filtering using adopt filter.

The presence of precipitable water vapour in the atmosphere delays the microwave signals. The differential delays causes errors in the elevation data. Atmospheric corrections are implemented for the DEMs using the models reported by [4]. MERIS PWV is used for the corrections. It has been noticed that the corrections did not improve the results as the variation of PWV over desert is seen to be not significant.

The other possible sources of errors can be the penetration of microwaves into the soil medium. It is reported [8] that there is considerable spatial variation in rainfall rate. This is also confirmed by studying the spatial variation of soil moisture by [9] . Since there is no improvement after tropospheric corrections, the possible error sources can be the diffusion of phases due to differential penetration of microwaves in to soil medium. The patterns observed in Figures 3a, 3e and 3g may be due to penetration of the waves into moist soils. A detailed investigation needs to be carried out in this direction.

Finally the decorrelation of the phases with increase in day difference can be partly responsible for errors.

## 5 Conclusions

After a detailed investigation into the errors in DEM of repeat pass InSAR in terms of spatial and temporal variations, patterns etc., the following conclusions are gained:

- Spatial distribution of Water vapour is fairly constant over Burgan oil field, though there is a temporal variation.
- RMS error is not a true representation of the actual errors. The large errors in some pockets of the study area may not be reflected in the RMS errors due to their less population. In the present context, we are interested in such pockets.
- Three factors are investigated as responsible for errors in the DEMs namely PWV, Soil moisture and temporal decorrelation.
- PWV corrections to InSAR has no significant effect on the accuracy of DEM.
- Temporal decorrelation has some influence on the accuracy of the derived DEM. Up to day difference of 455 days, the errors are acceptable. Beyond this period, the errors in DEM steeply increase.
- Spatial and temporal variability of soil moisture has influence on the accuracy of DEM. This needs to be further investigated. This can be checked by installing some Corner Reflectors over the Burgan oil field. For the study and calibration of land subsidence over Burgan oil field, there is a planning of installing 25 corner reflectors all over the Burgan oil field.

**Acknowledgments.** The authors are thankful to European Space Agency (ESA) for sponsoring the project . (C1F:3807) and providing (ASAR and MERIS) data sets free of charge. Also thanks to Research Administration, Kuwait University for sponsoring this project (SP: 02/08).

## References

1. Zebker, H.A., Goldstein, R.M.: Topographic mapping from interferometric synthetic aperture radar observations. Journal of Geophysical Research 91(B5), 4993–4999 (1986)
2. Hanssen, R.F.: Radar interferometry: data interpretation and error analysis, vol. xviii, 308 p. Kluwer Academic, Dordrecht (2001)
3. Hanssen, R.F.: Atmospheric heterogeneities in ERS tendem SAR interferometry, 136 p. Delft University press, Delft (1998)
4. Li, Z.: Correction of atmospheric water vapour effects on repeat-pass SAR interferferometry using GPS, MODIS and MERIS data. Ph. D. thesis, Department of geomatic Engineering, University college London (2005)
5. Al Jassar, H.K., Rao, K.S., Sabbah, I.: A model for the retrieval and monitoring of soil moisture over desert area of Kuwait. International journal of remote sensing 27(1-2), 329–348 (2006)
6. Rao, K.S., Kumar, V.P.B., Al Jassar, H.K.: An iterative technique to estimate baseline parameters in SAR Interferometry, Kuwait. Journal of Science and Engineering 34(2a), 91–109 (2007)
7. Rao, K.S., Phalke, S.M., Sakalley, J., Al Jassar, H.K.: Assessment of Geo-coding and Height Accuracy of the DEM derived from preliminary data sets of X-ba-nd SRTM. Journal of the Indian Society of Remote Sensing 34(IV), 369–375 (2006)
8. Marc, P.M., Elfatih, A.B.E.: The Hydroclimatology of Kuwait: Explaining Variability of Rainfall at Seasonal and Interannual Timescales (2008), doi:10.1175/2008JHM952.1, http://ams.allenpress.com/perlserv/?request=get-abstract&doi=10.1175%2F2008JHM952.1&ct=1
9. Al Jassar, H.K., Rao, K.S.: Validation of soil moisture retrieval models of Aqua satellite (AMSR-E) over Kuwait desert area. International Journal of Remote Sensing (will appear in the issue of 2010)